# Photoluminescence of Barium Titanate and Barium Zirconate in Multilayer Disordered Thin Films at Room temperature†

**M. L. Moreira,*,‡ M. F. C. Gurgel,‡ G. P. Mambrini,‡ E. R. Leite,‡ P. S. Pizani,|| J. A. Varela,§ and E. Longo§**

*Laboratório Interdisciplinar de Eletroquímica e Cerâmica, Departamento de Química and Departamento de Física, Universidade Federal de São Carlos, P.O. Box 676, 13565-905, São Carlos - SP, Brazil, and Laboratório Interdisciplinar em Cerâmica, Departamento de Físico-químico, Instituto de Química, Universidade Estadual Paulista, P.O. Box 355, 14801-907, R. Francisco Degni, s/n, Bairro Quitandinha, Araraquara - SP, Brazil*

*Received: February 23, 2008; Revised Manuscript Received: April 26, 2008*

The emission of wide band photoluminescence showed a synergic effect on barium zirconate and barium titanate thin films in alternate multilayer system at room temperature by 488 nm exiting wavelength. The thin films obtained by spin-coating were annealed at 350, 450, and 550 °C for 2 h. The X-ray patterns revealed the complete separation among the $BaTiO_3$ and $BaZrO_3$ phases in the adjacent films. Visible and intense photoluminescence was governed by $BaZrO_3$ thin films in the multilayer system. Quantum mechanics calculations were used in order to simulate ordered and disordered thin films structures. The disordered models, which were built by using the displacement of formers and modifier networks, showed a different symmetry in each system, which is in accordance with experimental photoluminescence emission, thus allowing to establish a correlation among the structural and optical properties of these multilayered systems.

## 1. Introduction

Recently, much attention is focused on the photoluminescent (PL) properties of titanates and zirconates with a disordered perovskite structure. The main reason is the distinct potential of these materials for electro-optic applications.[1,2] The optical properties of disordered semiconductors are characterized by the presence of a broad PL band. This phenomenon is attributed to the electronic states inside the band gap,[3] which are the main defects for an intense PL response.[4,5] The presence of states inside the band gap was attributed to the formation of clusters such as $[ZrO_5]-[TiO_6]$ or $[ZrO_6]-[TiO_5]$ which decrease the gap's emission.[6,7] Hence, the decrease in gap energy is related to oxygen deficiency promoted by the distortion of formers and modifier networks.[6–9] Recently, $Ba(Zr_x,Ti_{1-x},)O_3$ (BZT) was chosen as an alternative material to PZT in the manufacture of bulk ceramic or thin films [10,11] because it is highly stable and lead-free. However, the literature contains few reports about its PL properties, especially those of BZ thin films.

Many efforts have been made for preparing $BaTi0_3$ thin films by different deposition techniques such as sputtering, [12] pulsed laser deposition, [13,14] and molecular beam epitaxy.[15] More recently, an alternative route, based on a method of chemical solution deposition, called complex polymerization route, has been successful used for growing thin films of several oxides. The most interesting advantages of this method, compared with physical deposition methods, are the high deposition rates and low operational cost, because no high vacuum and others expensive equipments are involved in the process. Some examples of thin films successfully deposited by the complex polymerization route are PZT,[16] $BaTiO_3$,[17] $SrTiO_3$,[18] $LiNbO_3$,[19] and $LaNiO_3$[20] films. In all cases, the proposed methodology allowed the production of stoichiometric films with excellent structural and electrical properties, comparable with samples prepared in other works. Pontes and co-workers also used this methodology to prepare $SrTiO_3/BaTiO_3$ and $PbTiO_3/PbZrO_3$ crystalline multilayer thin films.[21,22]

In this work, we present the role of order−disorder degree associated with symmetry changes to discuss the visible two-dimensional PL properties in disordered $BaZrO_3$ (BZ) and $BaTiO_3$ (BT) thin films, as well as those of an alternate BT/BZ multilayer system at room temperature.

## 2. Experimental Details

$BaZrO_3$ and $BaTiO_3$ thin films were prepared by the complex polymerization method.[17] In this method, metallic alkoxides were added into a citric acid solution in order to obtain a metallic citrate complex. Titanium isopropoxide and zirconium butoxide (Aldrich) were utilized for BZ and BT, respectively. After this, a stoichiometric amount of barium carbonate (Mallinckrodt) was added, followed by the addition of ethylene glycol to promote the polymerization reaction. Those polymeric resins were deposited by spin coating onto Si(l11) substrates by using a Chemat Technology KW-4B spin coater. The films were heat-treated at different temperatures, that is, 350, 450, and 550 °C for 2 h in air atmosphere.

Each deposited layer was subjected to all the treatment before the deposition of the next layer, and four layers were deposited in order to obtain films with the desired thickness of approximately 250 nm estimated by the ellipsometry measurements.

## 3. Characterizations and Computational Methods

The samples were characterized by X-ray diffraction (XRD, Rigaku DMax 2500) by using CuKa radiation. Data were

† Part of the special section for the "Symposium on Energetics and Dynamics of Molecules, Solids and Surfaces".

* Corresponding author. Tel: +55 16 3351 8214. fax: +55 16 3351 8350. E-mail:mlucio@liec.ufscar.br.

‡ Departamento de Química, Universidade Federal de São Carlos.

§ Instituto de Química, Universidade Estadual Paulista.

|| Departamento de Física, Universidade Federal de São Carlos.

10.1021/jp801610y CCC: $40.75 
Published on Web 07/01/2008

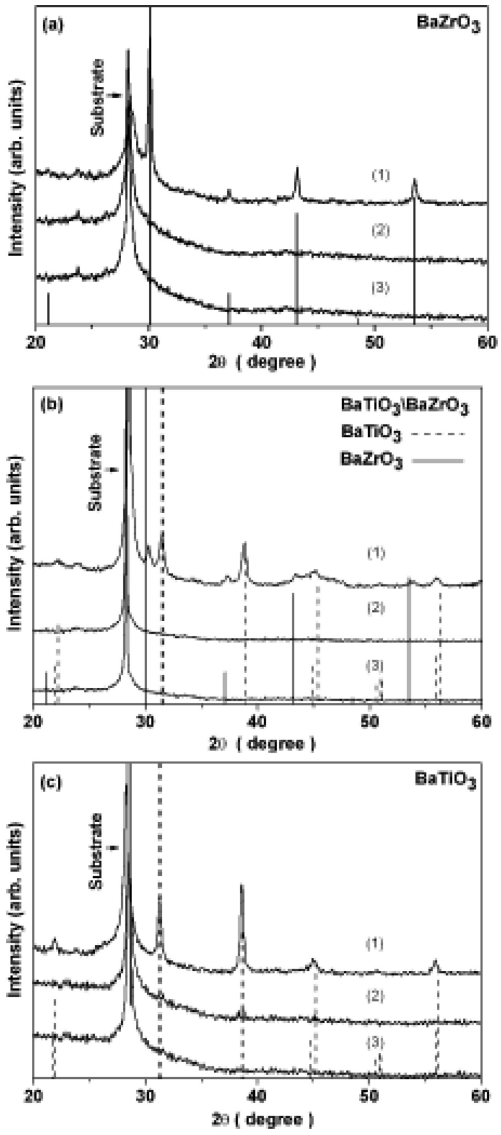


**Figure 1.** XRD patterns for (a) $BaZr0_3$, (b) $BaZr0_3/BaTi0_3$ multilayer system, and (c) $BaTi0_3$ thin films annealed at (1) 550 °C, (2) 450 °C, and (3) 350 °C for 2 h in air atmosphere.

collected from 20 to 60° in $2\theta$ range. The data were collected in fixed-time mode, with 0.02° step size and 1 s/point. Photoluminescence spectra of the thin films were taken with a U-1000 Jobin-Yvon double monochromator coupled to a cooled GaAs photomultiplier and a conventional photon counting system with 488.0 nm exciting and laser's maximum output power kept at 27 mW at room temperature. To gain a better understanding of the PL properties and their dependence on the structural order−disorder, the PL curves were analyzed by PickFit decovolution software.[23]

In this case, the ordered and disordered structures were compared individually by quantum mechanical calculations carried out with the CRYSTAL98 package,[24] which is based on both density functional theory and Hartree−Fock methods. The gradient-corrected correlation functional by Lee[25,26] was used, combined with the Becke3 exchange functional, B3LYP. Atomic centers have been described by all-electron basis sets 9763-311 (d631)G for Ba,[27] 976-31 (d62)G* for Zr,[27] 86-41 L(d31)G for Ti,[28] and 6-31G* for O.[28] Models for crystalline and distorted structures were built. These models were used to understand the PL by the ATOMDISP option of 0.5 Å

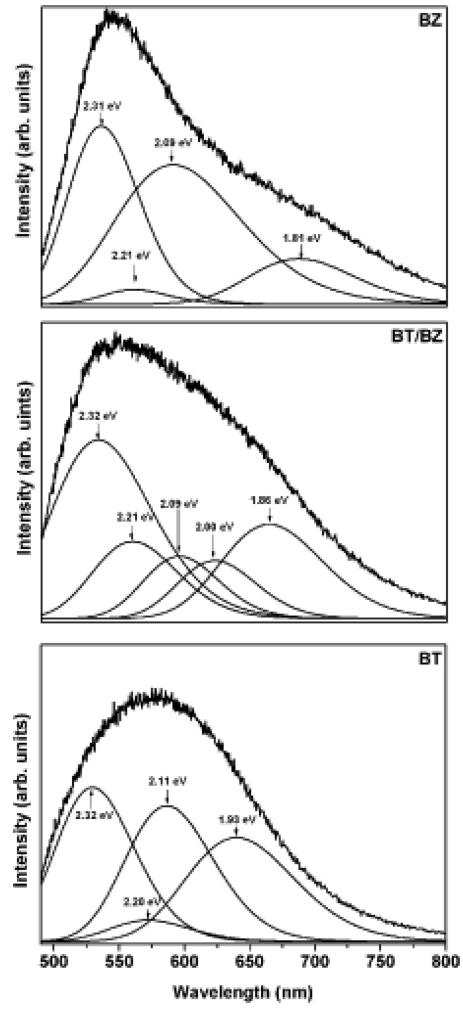


**Figure 2.** Deconvolution of PL spectra of BZ, BT/BZ, and BT thin films annealed at 350 °C for 2 h under air atmosphere.

displacements in the CRYSTAL98 package for the following atoms and associations: Ti, Zr, Ba, Ba−Ti, and Ba−Zr.

## 4. Results and Discussion

Figure 1 shows the XRD patterns of the samples deposited on Si(l11) substrates. In all cases, the films annealed at 350 and 450 °C have a disordered structure. This can be seen by the complete absence of diffraction peaks. The samples thermally treated at 550 °C are all crystalline ones. BT and BZ samples are single phase, indexed as a typical perovskite phase (JCPDS card no. 05-0626) with *P*4*mm* space group symmetry in tetragonal structure and (JCPDS card no. 06-0399) in *Pm*3*m* space group in cubic structure, respectively. In addition, there is no peaks related with $Ba(Ti,Zr)O_3$ solid solution phase. This results show that the proposed methodology allows the deposition of multilayer heterostructures without diffusion in the interfaces.

Photoluminescence of BZ and BT individual thin films at room temperature are reported in Figures 2 and 3 together with PL emission for BT/BZ multilayered thin films. In this figures, the indication of the a synergic effect between its thin films in multilayered systems annealed at 350 and 450 °C for 2 h can be observed. As these figures indicate, BZ films had a predominant effect on PL emission. Because the BZ films present a more intense photoluminescence than BT, it declines more quickly as shown in Figure 4. This PL effect was not

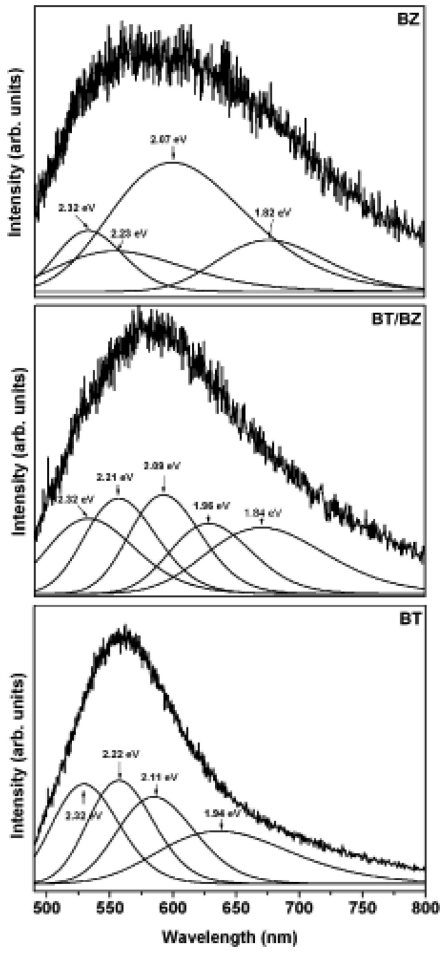


**Figure 3.** Decovolution PL spectra of BZ, BT/BZ, and BT thin films annealed at 450 °C for 2 h under air atmosphere.

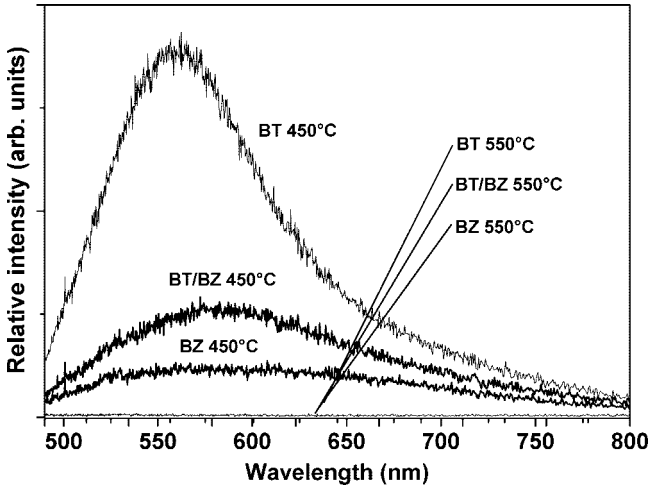


**Figure 4.** Evolution of photoluminescence spectra due to higher trend for structural order of BZ thin films in multilayered system annealed at 450 °C for 2 h under air atmosphere.

observed in BZ and/or BT powders.[6,29] Figures 2 and 3 depict the overall PL spectra and the decovolution in three distinct common bands, where the first maximum occurred at around 2.32 eV, followed by a maximum at 2.20 eV and one at 2.10 eV in all the thin films under study. A fourth uncommon band was observed at 1.80 eV in BZ films and at 1.93 eV in BT films.

The BT/BZ multilayer thin films showed five maxima in the common bands, with two occurring at 1.86 and at 1.99 eV.

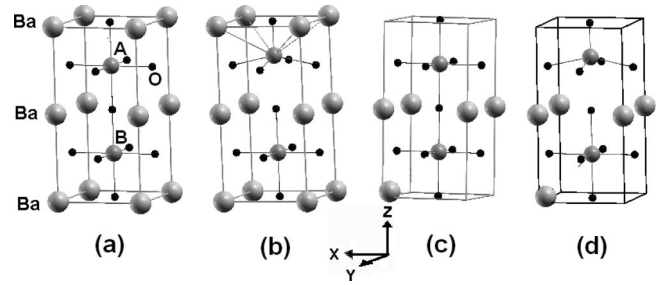


**Figure 5.** Structural models for (a) crystalline, (b) Ti and/or Zr, (c) Ba, and (d) Ba−Zr and/or Ba−Ti associations displacements performed with 0.5 A.

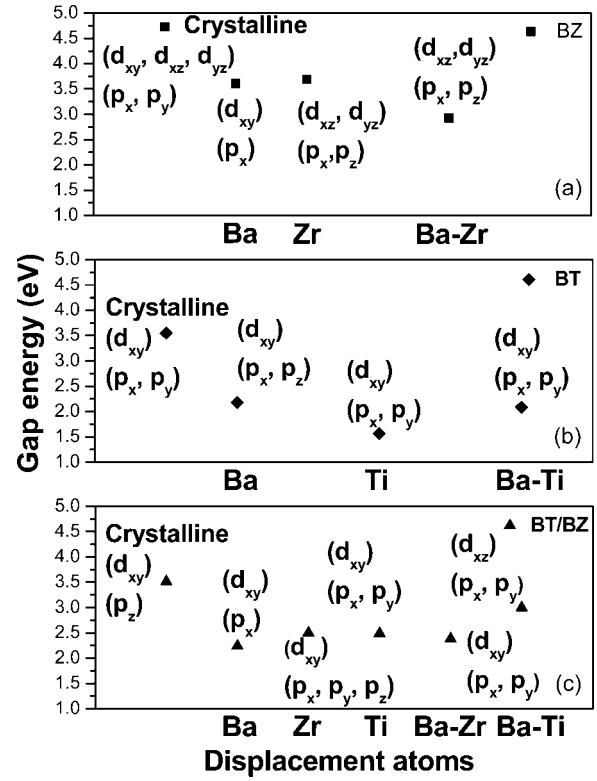


**Figure 6.** Dependence of energy gap on 0.5 A displacement for Ba, Ti, Zr, Ba−Zr, and Ba−Ti associations with the respective degenerate states in (a) BT, (b) BZ, and (c) BT/BZ multilayered thin films.

These two bands were in fact the ones observed in the isolated BT and BZ thin films, albeit displaced to a higher energy. This is an indication of almost perfect synergy between BT and BZ layers in the formation of photoluminescence because of superpositions of individual layer emission in multilayered system. The PL spectra of BT thin films depicted in Figures 2 and 3 are composed of two color components, the green component (maximum below 550 nm) and the yellow component (maximum below 623 nm). The BZ thin films, in turn, contain three color components: green, yellow, and red component (maximum below 710 nm). The PL spectrum of BT/BZ multilayer thin films is in fact a superposition of common and individual BT and BZ components. Each color represents a different type of electronic transition generated by different degrees of structural order−disorder[30] in each BT and BZ thin film in the multilayer system. The photoluminescence profile is typical of a multiphoton process, that is, an emission that occurs by several paths, involving numerous states within the forbidden band gap. These observations confirm the fact that PL is directly associated with the localized states existing inside of the band gap which are directly affected for degree of

order−disorder. Thus, when the structural order increases, the gap energy increases too.[31]

It is noted that both the excitation energy of 2.54 eV (488 nm) and the maximum profile emission centered around 2.1 eV for BT and 2.3 eV for BZ thin films are smaller than the band gap energy of highly ordered BT and BZ compounds, respectively. Therefore, there must exist certain localized levels within the forbidden band gap because the direct electron transition between the valence band and the conduction band should be not allowed.[30]

As one can see from Figure 5, no PL emission was observed for the thin films annealed at 550 °C for 2 h. One can also notice the predominant effect of BZ thin film on PL emission, which presents a higher trend for structural order than BT thin films when the annealing temperature increases. This fact is due to the increase of the structural order in these films and consequent reduction of the intermediate localized states inside the forbidden band gap.

Theoretical calculations were introduced with to better understand the creation of the states whitin the band gap. For this, the displacement of network formers (Ti, Zr) and/or network modifiers (Ba) promotes changes in symmetry, generating intermediate states inside the band gap for each displacement in each thin film.[31] These displacements can be associated with the breaking of bonds (Zr−O), (Ti−O) and/or (Ba−O), the formation of complex vacancies such as $V_0^x$. Thus, the emission is described as electron−hole recombination of a localized states in a no-regular octahedron [$TiO_6$−$TiO_5$, $ZrO_6$−$ZrO_5$, and/or $BaO_{12}$−$BaO_{11}$ complex clusters],[5,32,33] associated with structural disorder in BT, BZ, and BT/BZ multilayer thin films by the following equations.

$$[TiO_6]^x + [TiO_5V_0^x] \rightarrow [TiO_6]' + [TiO_5V_0^\bullet] \quad (1)$$

$$[TiO_6]^x + [TiO_5V_0^\bullet] \rightarrow [TiO_6]' + [TiO_5V_0^{\bullet\bullet}] \quad (2)$$

$$[ZrO_6]^x + [ZrO_5V_0^x] \rightarrow [ZrO_6]' + [ZrO_5V_0^\bullet] \quad (3)$$

$$[ZrO_6]^x + [ZrO_5V_0^\bullet] \rightarrow [ZrO_6]' + [ZrO_5V_0^{\bullet\bullet}] \quad (4)$$

$$[BaO_{12}]^x + [BaO_{11}V_0^x] \rightarrow [BaO_{12}]' + [BaO_{11}V_0^\bullet] \quad (5)$$

$$[BaO_{12}]^x + [BaO_{11}V_0^\bullet] \rightarrow [BaO_{12}]' + [BaO_{11}V_0^{\bullet\bullet}] \quad (6)$$

In this case, the $[TiO_5V_0^x]$, $[ZrO_5V_0^x]$, and $[BaO_{11}V_0^x]$ clusters are donor candidates. Besides, the $[TiO_6]^x$, $[ZrO_6]^x$, and $[BaO_{12}]^x$ clusters are acceptors candidates such as $[TiO_5V_0^\bullet]$, $[ZrO_5V_0^\bullet]$, and $[BaO_{11}V_0^\bullet]$. On the other hand, the $[TiO_5V_0^{\bullet\bullet}]$, $[ZrO_5V_0^{\bullet\bullet}]$, and $[BaO_{11}V_0^{\bullet\bullet}]$ are donor−acceptor candidates that were related by the displacement atoms in the structure such as that shown in Figure 5.

The models were simulated by using the CRYSTAL98 program, and the ATOMDISP option was used to provide the atomic displacements in the structure. Four different periodic models were built for BZ, BT, and BT/BZ. The atoms in ordered and disordered models are designed as A = B = Ti and Zr for BT and BZ models, respectively, and A = Ti and B = Zr for BT/BZ models.

The first model represents the ordered structure (crystalline) for BZ and BT models (see Figure 5a). The three others periodic models describe the disordered structure for BZ, BT, and BT/BZ models. These were simulated by displacement of the zirconium in direction *z* (see Figure 5b), barium in the diagonal direction (see Figure 5c), and zirconium−barium simultaneously (see Figure 5d) for BZ, BT, and BT/BZ models, respectively. The Zr, Ti, and Ba atoms were displaced by 0.5 Å in the *z* and diagonal (0.5, 0.5, 0.5) directions.

Figure 5a shows the symmetry structure for BZ, BT, and BT/BZ models, and figure **5**b−d illustrates the structural disorder for BZ, BT, and BT/BZ models. The asymmetric models were designed by displacement of the network former (Zr) and modifier (Ba). This displacement can be associated with three types of mechanisms involving oxygen vacancies that generate synergy in the system: $V_O^x$, $V_O^\bullet$, and $V_O^{\bullet\bullet}$. These defect mechanisms in the BZ, BT, and BT/BZ systems were simulated by displacement of the Zr, Ti, and Ba atoms together and separately to reproduce a disordered system or structural asymmetry.

The gap energy values (eV) for each model investigated can be analyzed in Figure 6. Theses gap values were obtained by theoretical results of level energy for atomic orbital oxygen in the top valence band and in the bottom conduction band for atomic orbital titanium or/and zirconium. The gap value

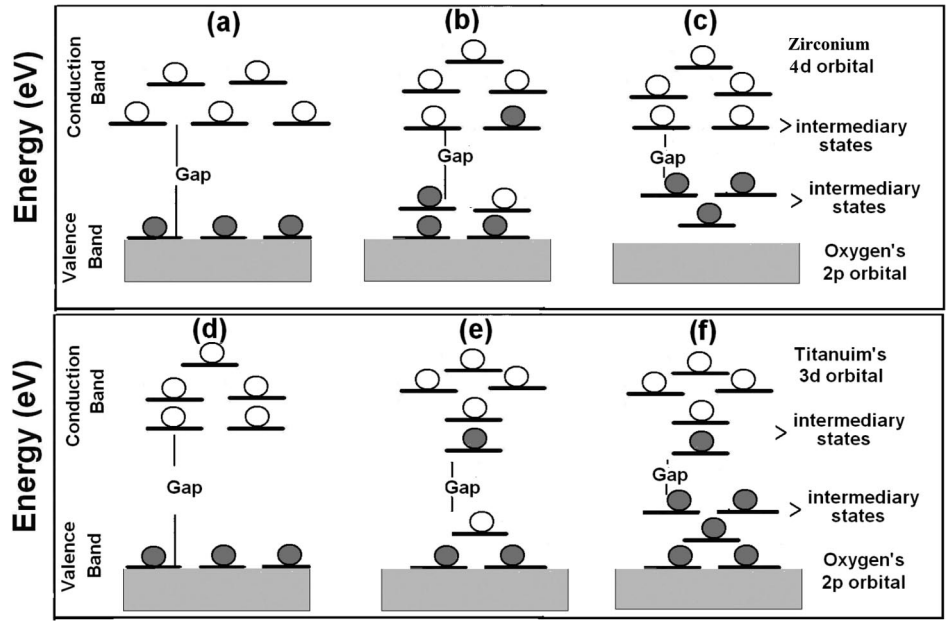


**Figure 7.** Model of energy state diagrams for (a and d) crystalline, (b and e) formation ions grid displacement, (c and f) former and modifier networks displacement in cubic and tetragonal structure, respectively.

difference for each model can be associated with the type of structural asymmetry or defects. In these models, the Jahn−Teller effect occurs, and the structural asymmetry induces the destabilization of atomic orbital of the oxygen atoms that results in the reduction of the gap values. This fact is responsible for the photoluminescence properties because it favors the appearance of small polarons in the gap region.

According to the hypothesis of Korzhik et al.,[34] there are vacant localized states linked to local defects such as oxygen vacancies in the band gap above the valence band and below the conduction band. In the Leonelli and Brebner[35] model, some electrons are promoted to the conduction band by absorption of photon creating small polarons. The polarons interact with holes trapped in the crystal (defects or impurities) and form self-trapped excitons that contribute to the visible PL emission. In our model, the wild band model,[30] the most important events occur before excitation, in other words, before the photon's arrival. The deep and shallow oxygen complex clusters, described by eqs 1–6, can generate localized states in the band gap, Figure 7. Besides, the charge distribution in the cell is inhomogeneous, thus allowing the trapping of electrons. The localized levels are energetically distributed, so that various energies are able to excite the trapped electrons.[33]

The defects originating from the displacement of Ti, Zr, or Ba atoms and their associations promote the destabilization of those atomic orbitals as well as of the oxygen orbital (Jahn−Teller effect),[36] leading to the appearance of intermediate states inside the forbidden band gap, as illustrate in Figure 7. It is known from the literature that materials with disordered structure have smaller band gap energy values than crystalline ones, as observed in our quantum mechanics calculations.[37]

The increase of destabilization states in the band gap energy is due to a symmetry break, simulated by the displacement of network modifier or network former atoms. In figure 7, the states created in the forbidden band gap take the crystalline gap energy, Figure 7a,d, to the lower gap energy by displacement of former networks, Figure 7b,e, and by cumulative effect of the former and modifier networks displacement, Figure 7c,f. Thus, a more asymmetrical structure leads to lower band gap energy, which is congruent with the experimental PL.

## 5. Conclusions

In conclusion, the PL emission of BT or BZ thin films was attributed to structural disorders present in individual thin films and in alternate BT/BZ multilayered thin film systems. The BZ thin films are predominant in photoluminescence emission because of a greated trend to structural order than that of BT thin films. A synergic effect of these disordered layers in multilayer systems was observed experimentally in the PL spectra, which is in accord with the simulated break of symmetry resulting from the destabilization of atomic orbitals performed by atom displacements in these structures.

**Acknowledgment.** The authors thank the financial support of the Brazilian research financing institutions: CAPES, FAPESP, and CNPq.

## References and Notes

(1) Bouma, B.; Blasse, G. *J. Phys. Chem. Solids* **1995**, *56*, 261.
(2) Pizani, P. S.; Basso, H. C.; Lanciotti, F.; Baschi, T. M.; Pontes, F. M.; Longo, E.; Leite, E. R. *Appl. Phys. Lett.* **2002**, *81*, 253.
(3) Coby, G. D.; Tiedje, T.; Abeles, B.; Brooks, B.; Godestein, Y. *Phys. Rev. Lett.* **1981**, *47*, 1489.
(4) Sousa, I. A.; Gurgel, M. F. C.; Santos, L. P. S.; Góes, M. S.; Cava, S.; Cilence, M.; Rosa, I. L. V.; Paiva-Santos, C. O.; Longo, E. *Chem. Phy.* **2006**, *322*, 343.
(5) Orhan, E.; Zenati, A.; Gurgel, M. F. C.; Pontes, F. M.; Leite, E. R.; Varela, J. A.; Longo, E. *Phys. Rev. B.* **2005**, *71*, 085113.
(6) Cavalcante, L. S.; Gurgel, M. F. C.; Simões, A. Z.; Longo, E.; Varela, J. A.; Joya, M. R.; Pizani, P. S. *Appl. Phys. Lett.* **2007**, *90*, 011901.
(7) Freitas, G. F. G.; Nasar, R. S.; Cerqueira, M.; Melo, D. M. A.; Longo, E.; Varela, J. A. *Mater. Sci. Eng. A* **2006**, *434*, 19.
(8) Longo, E.; Orhan, E.; Pontes, F. M.; Pinheiro, C. D.; Leite, E. R.; Varela, J. A.; Pizani, P. S.; Boschi, T. M.; Lanciotti, F., Jr.; Beltran, A.; Andres, J. *Phys. Rev. B.* **2004**, *69*, 125115.
(9) Yoshihiro, T.; Kenji, K.; Nobuo, I.; Satoru, I. *Appl. Phys. Lett.* **2006**, *88*, 151903.
(10) Yu, Z.; Ang, C.; Guo, R.; Bhalla, A. S. *Appl. Phys. Lett.* **2002**, *81*, 1285.
(11) Dixit, A.; Majumder, S. B.; Katiyar, R. S.; Bhalla, A. S. *Appl. Phys. Lett.* **2003**, *82*, 2679.
(12) Ianculescu, A.; Despax, B.; Bley, V.; Lebey, T.; Gavrila, R.; Dragan, N. *J. Eur. Ceram. Soc.* **2007**, *27*, 1129.
(13) Garca, T.; Bartolo-Prez, P.; de Posada, E.; Pea, J. L.; Villagrn-Muniz, M. *Surf. Coat. Technol.* **2006**, *27*, 3621.
(14) Qu, B. D.; Evstigneev, M.; Johnson, D. J.; Prince, R. H. *Appl. Phy. Lett.* **1998**, *72*, 1394.
(15) Yoneda, Y.; Sakaue, K.; Terauchi, H. *Surf. Sci.* **2003**, *529*, 283.
(16) Escote, M. T.; Pontes, F. M.; Leite, E. R.; Longo, E.; Jardim, R. F.; Pizani, P. S. *J. Appl. Phys.* **2004**, *96*, 2186.
(17) Lee, E. J. H.; Pontes, F. M.; Leite, E. R.; Longo, E.; Varela, J. A.; Araujo, E. B.; Eiras, J. A. *J. Mater. Sci. Lett.* **2000**, *19*, 1457.
(18) Pontes, F. M.; Leite, E. R.; Lee, E. J. H.; Longo, E.; Varela, J. A. *J. Eur. Ceram. Soc.* **2001**, *21*, 419.
(19) Bouquet, V.; Bernardi, M. I. B.; Zanetti, S. M.; Leite, E. R.; Longo, E.; Varela, J. A.; Viry, M. G.; Perrin, A. *J. Mater. Res.* **2000**, *15*, 2446.
(20) Escote, M. T.; Pontes, F. M.; Mambrini, G. P.; Leite, E. R.; Varela, J. A.; Longo, E. *J. Eur. Ceram. Soc.* **2005**, *25*, 2341.
(21) Pontes, F. M.; Leite, E. R.; Lee, E. J. H.; Longo, E.; Varela, J. A. *Thin Solid Films* **2001**, *385*, 260.
(22) Pontes, F. M.; Longo, E.; Leite, E. R.; Varela, J. A. *Appl. Phy. Lett.* **2004**, *84*, 5470.
(23) Ding, T.; Zheng, W. T.; Tian, H. W.; Zang, J. F.; Zhao, Z. D.; Yu, S. S.; Li, X. T.; Meng, F. L.; Wang, Y. M.; Kong, X. G. *Solid State Commun.* **2004**, *232*, 815.
(24) Saunders, V. R.; Dosevi, R.; Roetti, C.; Causa, M.; Harrison, N. M.; Zicovich-Wilson, C. M. *CRYSTAL98 user's manual*; University of Torino: Torino, 1998.
(25) Lee, C.; Yang, W.; Parr, R. G. *Phys. Rev. B* **1988**, *37*, 785.
(26) Becke, A. D. *J. Chem. Phys.* **1993**, *98*, 5648.
(27) http://www.tcm.phy.cam.ac.uk/^mdt26/crystal.html.
(28) http://www.crystal.unito.it/Basis_Sets/Ptable.html
(29) Pontes, F. M.; Escote, M. T.; Escudeiro, C. C.; Leite, E. R.; Longo, E.; Chiquito, A. J.; Pizani, P. S.; Varela, J. A. *J. Appl. Phys.* **2004**, *96*, 4386.
(30) Longo, V. M.; Cavalcante, L. S.; de Figueiredo, A. T.; Santos, L. P. S.; Longo, E.; Varela, J. A.; Sambrano, J. R.; Parkocimas, C. A.; De Vicente, F. S.; Hernades, A. C. *Appl. Phys. Lett.* **2007**, *90*, 091906.
(31) Leite, E. R.; Paris, E. C.; Pontes, F. M.; Paskocimas, C. A.; Longo, E.; Sensatoc, F.; Pinheiro, D.; Varela, J. A.; Pizani, P. S.; Campos, C. E. M.; Lanciotti, F.; Cheeseman, J. R. *J. Mat. Sci.* **2003**, *38*, 1175.
(32) Pontes, F. M.; Pinheiro, C. D.; Longo, E.; Leite, E. R.; Lazaro, S. R.; Maynani, R.; Pizani, P. S.; Boshi, T. M.; Lanciotti, F. *J. Lumin.* **2003**, *104*, 175.
(33) de Lazaro, S.; Milanez, J.; Figueiredo, A. T.; Longo, V. M.; Mastelaro, V. R.; Vicente, F. S.; Hernandes, A. C.; Varela, J. A.; Longo, E. *Appl. Phys. Lett.* **2007**, *90*, 111904.
(34) Korzhik, M. V.; Pavlenko, V. B.; Timoschenko, T. N.; Katchanov, V. A.; Singovskii, A. V.; Annenkov, A. N.; Ligum, V. A.; Solskii, I. M.; Peigneux, J. P. *Phys. Satus Solidi A* **1996**, *154*, 779.
(35) Leonelli, R.; Brebner, J. L. *Phys. Rev. B* **1986**, *33*, 8649.
(36) Orhan, E.; Pontes, F. M.; Leite, E. R.; Pizani, P. S.; Varela, J. A.; Longo, E. *ChemPhysChem* **2005**, *6*, 1530.
(37) Sambrano, J. R.; Orhan, E.; Gurgel, M. F. C.; Campos, A. B.; Ges, M. S.; Paiva-Santos, C. O.; Varela, J. A.; Longo, E. *Chem. Phys. Lett.* **2005**, *402*, 491.

JP801610Y